J. Fluid Mech. (2020), *vol.* 893, A12.
Published by Cambridge University Press

doi:10.1017/jfm.2020.225

Analytical solutions and virtual origin corrections for forced, pure and lazy turbulent plumes based on a universal entrainment function

F. Ciriello[1] **and G. R. Hunt**[1,†]

[1]Department of Engineering, University of Cambridge, Trumpington St., Cambridge CB2 1PZ, UK

(Received 27 June 2019; revised 12 December 2019; accepted 16 March 2020)

Previous measurements and numerical simulations of buoyant turbulent plumes that develop from area sources provide convincing evidence that entrainment varies locally in response to an imbalance from the asymptotic state of equilibrium, a state referred to as a pure plume. Across the wide spectrum of possible source conditions, that span forced and lazy plume releases, this variation of entrainment has been successfully captured by a single, or universal, description in which the entrainment function α varies linearly with the local Richardson number. Herein, an analytical solution for the virtual origin of forced, pure and lazy turbulent plumes from circular sources in unstratified environments is derived based on this universal description of entrainment. Prior to this, the analytical solutions reported were limited to those based on the simplifying assumption of invariant entrainment, so-called constant-α solutions of the plume conservation equations. Analytical solutions for the fluxes of volume and specific momentum are first developed. These solutions highlight the deficit in near-field entrainment in forced plumes and enable the general imbalance from the equilibrium state to be predicted via the streamwise variation of the local Richardson number. Focus then turns to the virtual origin due to the practical benefits that a knowledge of this location offers experimentalists (e.g. in comparing measurement with theory) and theoretical modellers (e.g. in incorporating a turbulent plume within a broader modelling framework).

Key words: plumes/thermals

1. Introduction

The classic framework for the theoretical study of turbulent plumes and the widely adopted model that captures the streamwise variation in plume entrainment were reported in the mid-twentieth century (Priestley & Ball 1955; Morton, Taylor & Turner 1956). However, until now, analytical solutions for turbulent plumes with such variable entrainment have eluded us. In this paper, we develop these solutions, solving directly the plume conservation equations subject to a local variability in entrainment.

† Email address for correspondence: gary.hunt@eng.cam.ac.uk

The applicability of the solutions we provide for the mean fluxes of volume and momentum is wide, spanning forced, pure and lazy plume releases. These solutions are complemented by expressions for the location of the virtual origin and insights into the streamwise variation of the Richardson number (§ 2). The close agreement we observe between these predictions and measurements of the virtual origin inferred from experiments (§ 3) provides confidence in their practical application.

Turbulence in a buoyant plume approaches a state of local equilibrium with height (Turner 1986). This state of equilibrium, referred to as a 'pure' plume (Morton 1959), allows for straightforward mathematical descriptions of turbulent entrainment that are based on self-similarity, i.e. on parameterisations of mixing that are locally invariant. This parameterisation forms the basis for the closure of the plume conservation equations of Morton *et al.* (1956) whose solutions have been used to predict the dynamics of turbulent plumes in nature, industry and the built environment (see the reviews by Kaye (2008), Woods (2010) and Hunt & van den Bremer (2011)).

For the pure plume, a height-invariant description of entrainment has legitimately been assumed and analytical solutions to these equations widely reported (Morton 1959; Morton & Middleton 1973; Hunt & Kaye 2001, 2005). Pure plumes do not exhibit a dynamical variability with height (Ezzamel, Salizzoni & Hunt 2015), their behaviour characterised by a local Richardson number $Ri(z)$ which maintains the unique pure-plume source value $Ri(z) = Ri_p$ at all heights $z \geqslant 0$; z denotes the vertical coordinate with origin coincident with the physical source and Ri_p the (constant) pure-plume Richardson number. These solutions treat the plume as self-similar at all distances from the source; this is satisfied only when the release is 'pure' (Turner 1986; Hunt & Kaye 2005), beyond the near-source region of flow establishment (Fischer *et al.* 1979).

Plumes from general (i.e. non-pure plume) area sources, however, are released such that the local conditions are distinct from those that characterise the self-similar state (Turner 1986). These plumes are in a 'non-pure' state, either locally 'forced' or 'lazy', and undergo an adjustment between the source and the far field (Morton 1959; Morton & Middleton 1973). The buoyancy force drives this adjustment and consequently there is dynamical variability, characterised by $Ri(z) \to Ri_p$, so that local conditions in the plume, including entrainment, are expected to depend on $Ri(z)$. This behaviour has been confirmed by measurements, in both thermal and aqueous-saline plumes, that show these imbalances radically change the entrainment in the proximity of the source and the approach to the self-similar state (Papanicolaou & List 1988; Wang & Law 2002; Kaye & Hunt 2009; Ezzamel *et al.* 2015). Further support for modified entrainment due to non-pure-plume behaviour has been garnered from direct numerical simulation (DNS) and theoretical studies (van Reeuwijk *et al.* 2016; Marjanovic, Taub & Balachandar 2017).

Studies on turbulent plumes spanning over 60 years of research are aligned in their view that entrainment for non-pure plumes varies as a linear function of the local Richardson number (Priestley & Ball 1955; Papanicolaou & List 1988; Wang & Law 2002; Kaminski, Tait & Carazzo 2005; Ezzamel *et al.* 2015; van Reeuwijk & Craske 2015). Beginning with Priestley & Ball (1955), entrainment was modelled by invoking this form for the case of a forced plume ($Ri(z) < Ri_p$), wherein a linear entrainment function $\alpha = \alpha(Ri(z))$ was introduced and matched between values measured for the pure jet and the pure plume. More recently, the same form for the entrainment function was deduced based on solutions of the plume conservation equations which are consistent with the equations for the conservation of energy fluxes (Kaminski *et al.* 2005; van Reeuwijk & Craske 2015). On account of these developments placing no

restrictions on the source condition for the plume, we have referred to this linear entrainment function as being universal. Surprisingly, despite the wide acceptance of this form, analytical solutions to the plume conservation equations subject to a linear dependence of the entrainment function with Richardson number have not previously been reported. Our motivation herein is therefore twofold: (i) to develop analytical solutions to the plume conservation equations for entrainment following a linear variation with local Richardson number and (ii) to determine the associated locations of the virtual origin for general forced, pure and lazy plumes from area sources.

The virtual origin refers to the location at which a point source of buoyancy flux would give rise to a plume whose behaviour matches the far-field behaviour of the actual (area source) plume of interest. In essence, the virtual origin is deduced as a vertical offset, or correction, to the analytical solutions for a plume formed from a point source of buoyancy flux. Hunt & Kaye (2001) provide a theoretical description of the origin location based on the solution to the plume equations for $\alpha = \text{constant}$. Whilst origin corrections are often instrumental in theoretical developments for which the plume is a single component of the overall system (Kaye & Hunt 2007), the magnitude of this correction and its dependence on the source conditions have not been determined for the aforementioned linear entrainment model.

The remainder of this paper is structured as follows. In § 2 analytical solutions are derived for a plume from a point source and a general area source. We then develop expressions for the virtual origin, make comparisons with laboratory measurements (§ 3), and discuss the insights these solutions provide regarding the approach of the plume to the self-similar state. Conclusions are drawn in § 5.

2. Solutions to the plume equations

Denoting z as the vertical coordinate with origin at the physical source, the steady integral conservation equations of Morton *et al.* (1956) for the time-averaged fluxes of volume πQ, specific momentum πM and buoyancy πB of an axisymmetric plume in an unstratified and otherwise quiescent environment may be expressed as

$$\frac{\mathrm{d}Q}{\mathrm{d}z} = 2\alpha M^{1/2}, \quad \frac{\mathrm{d}M}{\mathrm{d}z} = \kappa \frac{BQ}{M}, \quad \frac{\mathrm{d}B}{\mathrm{d}z} = 0, \tag{2.1a–c}$$

where $\kappa = 1$ for top-hat and $\kappa = 2$ for Gaussian profiles of buoyancy and vertical velocity. A derivation of (2.1) is given, for example, in Hunt & van den Bremer (2011). Following classic plume theory, the solution to these governing equations relies on a turbulence closure, known as the entrainment hypothesis, which relates the horizontal velocity of the fluid entrained peripherally into the plume u_e to a local vertical velocity w

$$u_e := \alpha w. \tag{2.2}$$

Widely referred to as the entrainment coefficient, herein we refer to α as the entrainment function (cf. Marjanovic *et al.* 2017) as we acknowledge that α may be constant or take a functional form depending on the source conditions. The assumption of a constant α relies on the spatial invariance of the local turbulence as achieved when there is a specific balance of the buoyancy and inertial forces acting on the flow (Turner 1986). Following Turner (1973), the ratio of these forces, whether in balance or otherwise, is characterised locally by the Richardson number

$$Ri(z) := \frac{BQ^2(z)}{M^{5/2}(z)}. \tag{2.3}$$

Regardless of the conditions imposed at source, all plumes naturally tend to a pure-plume self-similar state with streamwise distance z in which the local Richardson number is invariant, i.e. $Ri(z) \to Ri_p = \text{constant}$ as $z \to \infty$ (Morton 1959; Hunt & Kaye 2001). It follows, from (2.1) and (2.3), that the vertical variation of the Richardson number is

$$\frac{\mathrm{d}Ri}{\mathrm{d}z} = \left(4\alpha Ri - \frac{5\kappa}{2}Ri^2\right)\frac{M^{1/2}}{Q}. \tag{2.4}$$

Morton *et al.* (1956) deduced power-law solutions for the fluxes Q and M for the point-source plume, i.e. solving (2.1) subject to the source conditions $Q_0 = M_0 = 0$ and $B_0 > 0$ at $z = 0$. Morton (1959) then extended the analysis to area sources. He demonstrated that these plumes may be characterised by a scaled source Richardson number

$$\Gamma_0 := \frac{Ri_0}{Ri_p} \quad \text{where } Ri_0 = \frac{B_0 Q_0^2}{M_0^{5/2}}. \tag{2.5}$$

For non-pure source conditions, i.e. $Ri_0 \neq Ri_p$, the source fluxes create an imbalance from the pure-plume state in the proximity of the source, where locally the scaled Richardson number $\Gamma(z) := Ri(z)/Ri_p \neq 1$. Morton (1959) presented approximate solutions to (2.1) for $0 < \Gamma_0 < 1$ (so-called forced plumes) based on a vertical offset to the pure-plume power-law solutions; these vertical offsets being widely referred to as virtual origin corrections. Morton & Middleton (1973) extended his analysis to plumes from sources for which $\Gamma_0 > 1$ (so-called lazy plumes). Hunt & Kaye (2001) subsequently deduced analytical solutions for the plume fluxes and virtual origin valid for both forced and lazy cases. The aforementioned solutions are all based on the assumption of a constant value of α and thus do not take into account changes in behaviour due to imbalances from pure-plume behaviour.

2.1. *The entrainment function*

Non-pure plumes that are formed from area sources do not exhibit spatially invariant turbulence and are characterised by a vertical variation of the local Richardson number, from a source value of Ri_0 to the far-field value of Ri_p (Turner 1986). Several analyses of the derivation of the plume conservation equations, including those of Priestley & Ball (1955), Kaminski *et al.* (2005) and van Reeuwijk & Craske (2015), have shown that the entrainment function takes the form

$$\alpha := \gamma_1 + \gamma_2 Ri, \tag{2.6}$$

for constant coefficients $\gamma_1 > 0$ and $\gamma_2 > 0$. Table 1 summarises historical numerical predictions and experimental measurements of these coefficients. The solution of (2.1*c*) is $B = B_0$ irrespective of the entrainment function. Carazzo, Kaminski & Tait (2006) propose an extended form of (2.6) that compensates for the adjustment of the cross-stream velocity and buoyancy profiles with streamwise distance (see discussion in appendix A). Invoking the entrainment function (2.6), the conservation equations (2.1*a*,*b*) become

$$\frac{\mathrm{d}Q}{\mathrm{d}z} = 2\gamma_1 M^{1/2} + 2\gamma_2 B_0 \frac{Q^2}{M^2}, \quad \frac{\mathrm{d}M}{\mathrm{d}z} = \kappa B_0 \frac{Q}{M}. \tag{2.7a,b}$$

Author(s)		Top-hat ($\kappa = 1$)			Gaussian ($\kappa = 2$)			Approach
		γ_1	γ_2	α_p	γ_1	γ_2	α_p	
Rouse, Yih & Humphreys (1952)	P	—	—	0.116	—	—	0.082	Hot wire
Priestley & Ball (1955)	F	0.071	0.35	0.127	0.05	0.25	0.09	Thermocouple
Morton *et al.* (1956)	P	—	—	0.131	—	—	0.093	Filling-box
Baines (1983)	P	—	—	0.103	—	—	0.073	Filling-box
Papanicolaou & List (1988)	F	0.078	0.25	0.117	0.055	0.18	0.083	LDV
Wang & Law (2002)	F	0.075	0.25	0.125	0.053	0.18	0.088	PIV
Kaminski *et al.* (2005)	F	0.085	0.35	0.140	0.060	0.25	0.099	dye
Ezzamel *et al.* (2015)	F	0.075	0.51	0.156	0.053	0.36	0.110	PIV
van Reeuwijk *et al.* (2016)	J	0.091	—	—	0.064	—	—	DNS
	F	0.085	0.25	0.127	0.060	0.25	0.090	DNS
	P	0.095	0.20	0.137	0.067	0.20	0.097	DNS
Marjanovic *et al.* (2017)	L	0.085	0.24	0.139	0.060	0.24	0.098	DNS
Average	—	0.082	0.34	0.129	0.060	0.24	0.091	—
$\pm 2\sigma$	—	0.016	0.16	0.014	0.011	0.12	0.020	—

TABLE 1. Values for γ_1 and γ_2 in axisymmetric plumes. Entries for the pure-plume entrainment coefficient α_p are given. The letters P, J, F and L are indicative of plume behaviour in each study. P indicates a pure plume, J a pure jet, F a forced plume and L a lazy plume. Hereafter, we take the average values listed. LDV (laser-Doppler velocimetry). PIV (particle image velocimetry).

2.2. *Point-source solution*

For the point source, $Q_0 = M_0 = 0$ at $z = 0$. Thus, guided by dimensional considerations, we seek the power-law solutions

$$Q = C_Q B_0^{1/3} z^{5/3}, \quad M = C_M B_0^{2/3} z^{4/3}. \tag{2.8a,b}$$

Substituting (2.8) into (2.7) yields the coefficients

$$C_Q = \frac{4}{3\kappa}\left(\frac{9\gamma_1\kappa^2}{10\kappa - 16\gamma_2}\right)^{4/3}, \quad C_M = \left(\frac{9\gamma_1\kappa^2}{10\kappa - 16\gamma_2}\right)^{2/3}. \tag{2.9a,b}$$

2.3. *Area-source solution*

For the general area-source conditions $Q_0 > 0$, $M_0 > 0$ and $B_0 > 0$, we scale Q and M on their respective source values and the streamwise coordinate on $L_q := Q_0/M_0^{1/2}$. Thus, we introduce

$$\zeta := \frac{z}{L_q}, \quad q := \frac{Q}{Q_0}, \quad m := \frac{M}{M_0}. \tag{2.10a–c}$$

Note, for top-hat profiles, L_q is the radius of the source. Accordingly, (2.7) reduce to

$$\frac{\mathrm{d}q}{\mathrm{d}\zeta} = 2\gamma_1 m^{1/2} + 2\gamma_2 Ri_p \Gamma_0 \frac{q^2}{m^2}, \quad \frac{\mathrm{d}m}{\mathrm{d}\zeta} = \kappa Ri_p \Gamma_0 \frac{q}{m}, \tag{2.11a,b}$$

where the pure-plume Richardson number is given by

$$Ri_p = \frac{8\gamma_1}{5\kappa - 8\gamma_2} \left(= \frac{C_Q^2}{C_M^{5/2}} \right). \tag{2.12}$$

Combining (2.11*a*) and (2.11*b*) gives the nonlinear differential equation

$$\frac{\mathrm{d}q}{\mathrm{d}m} = \frac{2\gamma_1}{\kappa Ri_p \Gamma_0} \frac{m^{3/2}}{q} + \frac{2\gamma_2}{\kappa} \frac{q}{m}. \tag{2.13}$$

Defining $\mathscr{A}_1(m) := 2\gamma_1 m^{3/2}/\kappa Ri_p \Gamma_0$ and $\mathscr{A}_2(m) := -2\gamma_2/\kappa m$, (2.13) becomes

$$\frac{\mathrm{d}q}{\mathrm{d}m} = \mathscr{A}_1(m) q^{-1} - \mathscr{A}_2(m) q. \tag{2.14}$$

This is the Bernoulli differential equation for which solutions are readily available (Ince 1956, pp. 22–23). With the change of variable $\eta := q^2$, (2.14) reduces to the linear differential equation

$$\frac{\mathrm{d}\eta}{\mathrm{d}m} = 2q \frac{\mathrm{d}q}{\mathrm{d}m} = A_1(m) - \eta A_2(m), \tag{2.15}$$

where $A_1(m) := 2\mathscr{A}_1(m)$ and $A_2(m) := 2\mathscr{A}_2(m)$. Writing c as a constant of integration, the solution of (2.15) is

$$\eta = \frac{\displaystyle\int \exp\left(\int A_2(m)\,\mathrm{d}m \right) A_1(m)\,\mathrm{d}m + c}{\displaystyle\exp\left(\int A_2(m)\,\mathrm{d}m \right)}. \tag{2.16}$$

Integrating from the source, where $q = 1$ and $m = 1$, the solution of (2.13) is thus

$$q^2 = \frac{\displaystyle 4\gamma_1 \int_1^m \exp\left(-\frac{4\gamma_2}{\kappa} \int_1^m \frac{1}{m}\,\mathrm{d}m \right) m^{3/2}\,\mathrm{d}m + 2c}{\displaystyle \kappa Ri_p \Gamma_0 \exp\left(-\frac{4\gamma_2}{\kappa} \int_1^m \frac{1}{m}\,\mathrm{d}m \right)}. \tag{2.17}$$

Performing the integration in (2.17) we have

$$q^2 = \frac{1}{\Gamma_0}(m^{5/2} - m^{4\gamma_2/\kappa}) + 2cm^{4\gamma_2/\kappa}. \tag{2.18}$$

From the source conditions, the constant of integration $c = 1/2$. As a result, (2.18) may be written as

$$q^2 = \frac{m^{5/2}}{\Gamma_0} + \frac{\Gamma_0 - 1}{\Gamma_0} m^{4\gamma_2/\kappa} \quad \Rightarrow \quad \Gamma = 1 + (\Gamma_0 - 1) m^{4\gamma_2/\kappa - 5/2}. \tag{2.19a,b}$$

The first term on the right-hand side of (2.19*a*) is the pure-plume component; note from the dimensionless form of (2.8) that $q^2 = m^{5/2}$ for $\Gamma_0 = 1$, and correspondingly from (2.19*b*), $\Gamma = 1$. The second term thus captures the adjustment towards

pure-plume behaviour. Note that the sign of the exponent on m is negative (e.g. $4\gamma_2/\kappa - 5/2 \approx -1.14$ taking $\gamma_2 = 0.34$ and $\kappa = 1$, table 1). Momentum flux increases monotonically with streamwise distance ζ due to the work done by the buoyancy force, thus from (2.19*b*) Γ asymptotes to a value of unity as expected.

Substituting for the physically realistic (positive) root for q from (2.19*a*) into (2.11*b*)

$$\frac{\mathrm{d}m}{\mathrm{d}\zeta} = \frac{\kappa Ri_p \Gamma_0}{m}\left(\frac{m^{5/2}}{\Gamma_0} + \frac{\Gamma_0 - 1}{\Gamma_0} m^{4\gamma_2/\kappa}\right)^{1/2}. \tag{2.20}$$

Hence

$$\zeta = \frac{1}{\kappa Ri_p \Gamma_0^{1/2}} \int_1^m m^{-1/4}(1 + (\Gamma_0 - 1)m^{4\gamma_2/\kappa - 5/2})^{-1/2}\,\mathrm{d}m. \tag{2.21}$$

Defining ${}_2F_1$ as the ordinary hypergeometric function (e.g. Abramowitz & Stegun 1964, pp. 556–566)

$${}_2F_1(a, b; c; x) = \sum_{n=0}^{\infty} \frac{a^{\underline{n}}\, b^{\underline{n}}}{c^{\underline{n}}} \frac{x^n}{n!}, \quad \text{where } a^{\underline{n}} = \prod_{k=0}^{n}(a - k), \tag{2.22a,b}$$

denotes the falling Pochhammer symbol, (2.21) can be integrated to give

$$\zeta = \frac{4}{3\kappa Ri_p \Gamma_0^{1/2}}(m^{3/4} + \mathscr{F} - \mathscr{F}_\delta), \tag{2.23}$$

where the functions $\mathscr{F} = \mathscr{F}(m, \Gamma_0)$ and $\mathscr{F}_\delta = \mathscr{F}_\delta(\Gamma_0)$ are defined as

$$\begin{aligned}\mathscr{F} &= {}_2F_1\left(\frac{1}{2}, \frac{3}{8\gamma_2/\kappa - 10}; 1 + \frac{3}{8\gamma_2/\kappa - 10}; (1 - \Gamma_0)m^{4\gamma_2/\kappa - 5/2}\right) - 1 \\ &= \sum_{k=0}^{\infty}\left(\frac{\displaystyle\prod_{k=0}^{n}\left(\frac{1}{2} - k\right)\prod_{k=0}^{n}\left(\frac{3}{8\gamma_2/\kappa - 10} - k\right)}{\displaystyle\prod_{k=0}^{n}\left(1 + \frac{3}{8\gamma_2/\kappa - 10} - k\right)} \frac{((1 - \Gamma_0)m^{4\gamma_2/\kappa - 5/2})^n}{n!}\right) - 1,\end{aligned} \tag{2.24}$$

and

$$\begin{aligned}\mathscr{F}_\delta &= {}_2F_1\left(\frac{1}{2}, \frac{3}{8\gamma_2/\kappa - 10}; 1 + \frac{3}{8\gamma_2/\kappa - 10}; 1 - \Gamma_0\right) \\ &= \sum_{k=0}^{\infty}\left(\frac{\displaystyle\prod_{k=0}^{n}\left(\frac{1}{2} - k\right)\prod_{k=0}^{n}\left(\frac{3}{8\gamma_2/\kappa - 10} - k\right)}{\displaystyle\prod_{k=0}^{n}\left(1 + \frac{3}{8\gamma_2/\kappa - 10} - k\right)} \frac{(1 - \Gamma_0)^n}{n!}\right).\end{aligned} \tag{2.25}$$

Asymptotically far from the source, the plume becomes pure, cf. (2.19*b*), and momentum flux scales with the 4/3rd power of distance, cf. (2.8*b*). Thus, an origin correction ζ_v can be deduced on rearranging (2.23) in the form

$$m = C_M Ri_p^{2/3} \Gamma_0^{2/3}(\zeta + \zeta_v)^{4/3} \quad \Rightarrow \quad \zeta_v = \frac{4}{3\kappa Ri_p \Gamma_0^{1/2}}(\mathscr{F}_\delta - \mathscr{F}). \tag{2.26a,b}$$

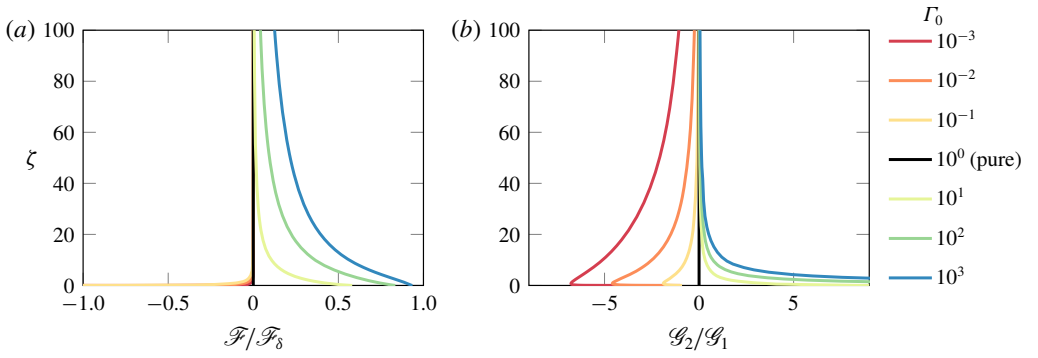

FIGURE 1. (*a*) Values of $\mathscr{F}/\mathscr{F}_\delta$ versus ζ and (*b*) $\mathscr{G}_2/\mathscr{G}_1$ versus ζ for different values of Γ_0.

In the limit as $\zeta \to \infty$, $\zeta_v \to \zeta_{avs}$, $(1-\Gamma_0)m^{4\gamma_2/\kappa-5/2} \to 0$ and $\mathscr{F} \to 0$, and hence (2.26*b*) reduces to

$$\zeta_{avs} = \frac{4}{3\kappa Ri_p \Gamma_0^{1/2}} \mathscr{F}_\delta. \tag{2.27}$$

The solution for the asymptotic virtual origin given in (2.27) is valid for forced, pure and lazy plumes, i.e. $\Gamma_0 > 0$. Figure 1(*a*) plots $\mathscr{F}/\mathscr{F}_\delta$ versus ζ confirming that $\mathscr{F} \ll \mathscr{F}_\delta$ for $\zeta \gg 1$.

While (2.27) remains the apex contribution of the current analysis, an alternative solution approach to determine ζ_{avs} is to expand the bracketed term in (2.21) using the binomial theorem and integrate term by term to give

$$\zeta_{avs} = \frac{3\mathscr{B}_\delta}{4\kappa Ri_p \Gamma_0^{1/2}}, \quad \mathscr{B}_\delta := \sum_{k=0}^{\infty} \frac{(\Gamma_0-1)^k}{k!(k(4\gamma_2-5/2)+3/4)} \prod_{j=1}^{k} \left(\frac{1}{2}-j\right). \tag{2.28a,b}$$

This solution, valid for $0 < \Gamma_0 < 2$, reduces to the constant-α solution of Hunt & Kaye (2001) on setting $\gamma_2 = 0$. Expressions (2.27) and (2.28*a*) scale identically on Ri_p and Γ_0 and indeed are identical in the range $0 < \Gamma_0 < 2$ (indicating that $3\mathscr{B}_\delta/4 = 4\mathscr{F}_\delta/3$).

Substituting for m from (2.26) into (2.19) gives the square of the volume flux

$$q^2 = \mathscr{G}_1 + \mathscr{G}_2 \quad \Rightarrow \quad q = \mathscr{G}_1^{1/2}\left(1+\frac{\mathscr{G}_2}{\mathscr{G}_1}\right)^{1/2}, \tag{2.29a,b}$$

where the functions $\mathscr{G}_1(\Gamma_0, \zeta)$ and $\mathscr{G}_2(\Gamma_0, \zeta)$ are defined as

$$\mathscr{G}_1 := \Gamma_0^{2/3} C_Q^2 Ri_p^{2/3} (\zeta+\zeta_v)^{10/3}, \tag{2.30}$$

$$\mathscr{G}_2 := \frac{\Gamma_0 - 1}{\Gamma_0^{1-8\gamma_2/3\kappa}} (C_Q^3 Ri_p)^{16\gamma_2/15\kappa} (\zeta+\zeta_v)^{16\gamma_2/3\kappa}. \tag{2.31}$$

Since $\mathscr{G}_2$ is associated with the non-pure adjustment behaviour, cf. (2.19*b*), the ratio $\mathscr{G}_2/\mathscr{G}_1 \to 0$ in the limit as $\zeta \to \infty$, provided $\gamma_2/\kappa \leqslant 5/8$, (n.b. which indeed is the case cf. table 1)

$$\frac{\mathscr{G}_2}{\mathscr{G}_1} = \frac{\Gamma_0 - 1}{\Gamma_0^{(1-8\gamma_2/\kappa)/3}} C_Q^{16(\gamma_2/\kappa-5/8)/5} Ri_p^{16(\gamma_2/\kappa-5/8)/15} (\zeta+\zeta_v)^{16(\gamma_2/\kappa-5/8)/3} \tag{2.32}$$

(see figure 1*b*).

Finally, substituting for m from (2.26*a*) into (2.19*b*), the variation of the local Richardson number $\Gamma(\zeta)$, indicating the imbalance from the equilibrium state, is

$$\Gamma(\zeta) = 1 + (\Gamma_0 - 1)((\Gamma_0 Ri_p)^{2/3} C_M)^{4(\gamma_2/\kappa - 5/8)} (\zeta + \zeta_v)^{16(\gamma_2/\kappa - 5/8)/3}. \tag{2.33}$$

3. Experiments

Particle image velocimetry measurements were acquired for negatively buoyant plumes formed by the injection of an aqueous-saline solution into a freshwater filled visualisation tank. Polyamide seeding particles with a nominal diameter of 50 μm and a density of 1.03 g cm^{-3} were used to seed the flow. PIV measurements were only conducted for plume release densities lower than 1.02 g cm^{-3} in order to minimise the optical distortion of particles owing to differences in refractive index between the saline release and the freshwater ambient. The Stokes velocity of the particles, estimated at 0.04 cm s^{-1}, was considerably smaller than the centreline velocities recorded in the plume (1–7 cm s^{-1}) such that the velocity lag experienced by the particles was expected to be minimal.

The videos were recorded at an acquisition rate of 30 f.p.s. with a shutter speed of 10 ms. A high aperture (F/1.4) was used to reduce the depth of field to a depth less than the thickness of the light sheet (the latter estimated at 10 mm). The PIV window was 180 × 360 mm^2 (width by height) recorded with a resolution of 5 Megapixels (2048 × 2560). Particle scatter size roughly ranged between 3 and 5 pixels. A 15 pixel highpass filter was used to improve uneven lighting and a 5 pixel Wiener denoise filter was applied to reduce ghosting due to noise and unfocused particles. A two-pass interrogation scheme was adopted. Interrogation windows of area 128 × 128 and 64 × 64 pixels^2 were used with a 50 % overlap for each window. Processing was conducted using a modified version of the open source software PIVlab from Thielicke & Stamhuis (2014).

Plume nozzles with 44.5 mm and 89.0 mm diameters were used. The volume flux was estimated by integrating the time-averaged velocity field measured along the central plume axis and assuming rotational symmetry. The source volume flux was measured with an Apollo LowFlo flowmeter, with range 0.1–3.0 l min^{-1}, and to an accuracy of ±1 % of the reading. The density of the saline solution and freshwater ambient was measured with an Anton Paar DMA 5000 density meter of accuracy ±0.0005 g cm^{-3}.

The virtual origin correction ζ_{v*} was estimated from the volume flux measurements by defining it as

$$\zeta_{v*} := \frac{q_*^{3/5}}{C_Q^{3/5} Ri_0^{1/5}} - \zeta_*, \tag{3.1}$$

where the asterisk subscript $(\cdot)_*$ denotes a measured quantity. The maximum cumulative error $|\delta\zeta_{v*}|$ on ζ_{v*} was estimated to be ±11 %. The error on $C_Q(\gamma_1, \gamma_2)$ was estimated based on the historical values of γ_1 and γ_2 reported in table 1. Our estimates of the location for the virtual origin from (3.1) are shown in what follows by circular markers (●) with error bars overlain.

4. Results and discussion

The solutions for the $\alpha = \text{constant}$ and $\alpha = \gamma_1 + \gamma_2 Ri$ formulations are expected to be indistinguishable in the far field, where locally the differences in behaviour between the actual plume and a pure plume are diminishingly small, irrespective of the source

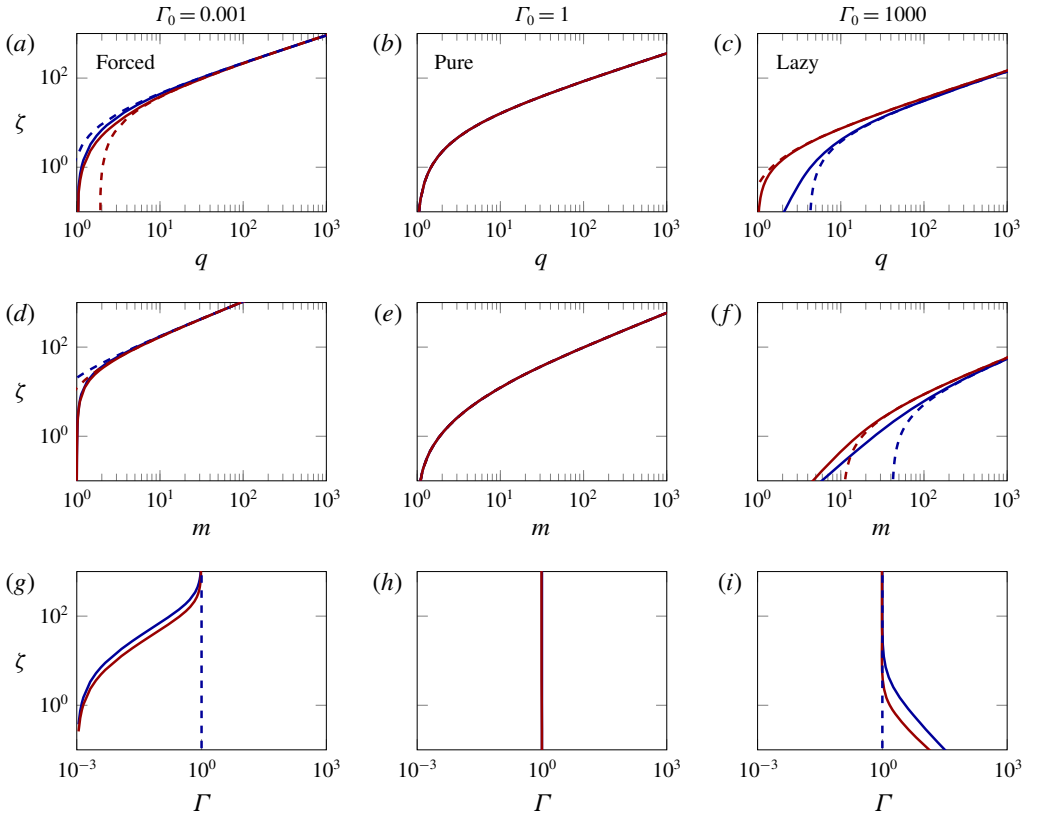

FIGURE 2. Values of q (*a–c*), m (*d–f*) and $\Gamma(\zeta)$ (*g–i*) versus ζ for $\Gamma_0 = \{0.001, 1, 1000\}$, highlighting differences between the analytical solutions for $\alpha =$ constant (solid red lines -) from Hunt & Kaye (2005), and for $\alpha = \gamma_1 + \gamma_2 Ri$ (solid blue lines -) from (2.29), (2.26) and (2.33) (top-hat, $\kappa = 1$). Corresponding dashed lines show approximate solutions based on the virtual origin corrections given by Hunt & Kaye (2001, dashed red lines - -) and by (2.27, dashed blue lines - -). The $\alpha =$ constant and $\alpha = \gamma_1 + \gamma_2 Ri$ solutions overlie for the pure-plume case.

conditions (2.19*b*). This is confirmed in figure 2, which plots the streamwise variations of volume flux (figure 2*a–c*, from (2.29)) and momentum flux (figure 2*d–f*, from (2.26)), for example cases of forced ($\Gamma_0 = 0.001$), pure ($\Gamma_0 = 1$) and lazy ($\Gamma_0 = 1000$) plumes. For the forced plume there is clearly a deficit in entrainment prevalent (lower volume flux) in the near-source region for the $\alpha = \gamma_1 + \gamma_2 Ri$ formulation (blue line) when compared with the constant-α predictions (red line); the trend in this region is reversed for lazy plumes. The variation of $\Gamma(\zeta)$ is plotted in figure 2(*g–i*). In both forced (figure 2*g*) and lazy (figure 2*i*) cases, the solutions indicate that the approach to pure behaviour is less rapid than predicted by constant-α solutions.

Our analytical solution (2.27) for the virtual origin correction $\zeta_{avs} = z_{avs}/L_q$, recalling $L_q = Q_0/M_0^{1/2}$, is plotted as a function of Γ_0 in figure 3(*a*) together with ζ_{avs} inferred from integrating (2.11) numerically using a fourth-order Runge–Kutta method. Numerical and analytical solutions overlie so as to be graphically indistinguishable. Evidently, agreement between the prediction ((2.27), blue line -) and the data is good

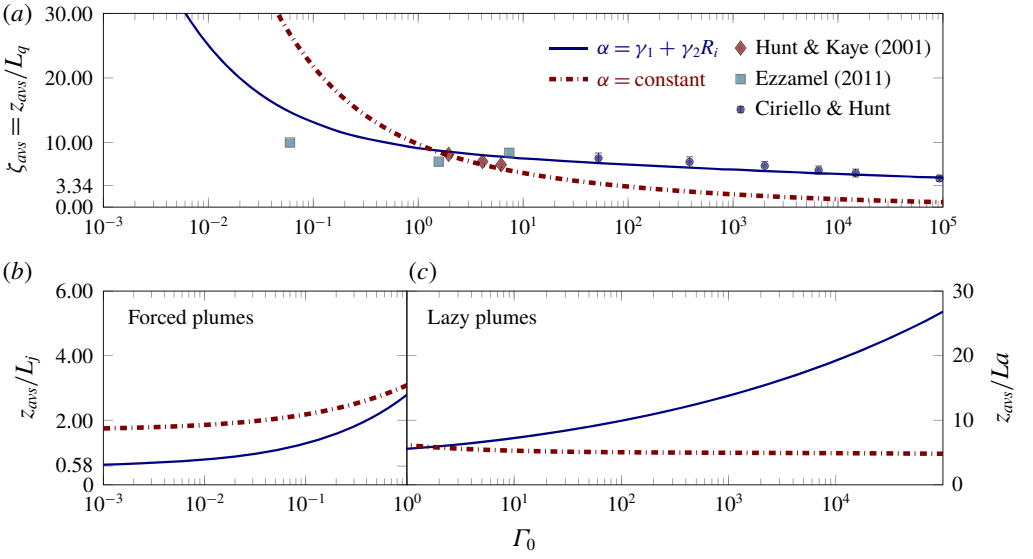

FIGURE 3. (*a–c*) Value of z_{avs} versus Γ_0 for $\kappa = 1$. Solution for $\alpha =$ constant from Hunt & Kaye (2001, dot-dashed red line -·-) and for $\alpha = \gamma_1 + \gamma_2 Ri$ from ((2.27), blue line -). Markers plotted in (*a*) show experimental measurements from Hunt & Kaye (2001, ◆), Ezzamel (2011, ■) and our own PIV measurements of aqueous-saline plumes (§ 3, ●).

and improved over the constant-α solution of Hunt & Kaye (2001, dot-dashed red line -·-).

Physically, the magnitude of the virtual origin correction is indicative of the characteristic streamwise length over which the adjustment towards the pure-plume-like state occurs (Hunt & Kaye 2001). Based on classically adopted scalings, the adjustment length is expected to scale on the jet length $L_j := M_0^{3/4}/B_0^{1/2} (\equiv L_q Ri_0^{-1/2})$ for forced plumes (Papanicolaou & List 1988; Wang & Law 2002), and on the acceleration length $L_a := Q_0^{3/5}/B_0^{2/5} (\equiv L_q Ri_0^{-1/5})$ for lazy plumes (Fischer *et al.* 1979; Hunt & Kaye 2005). To assess this, figure 3(*b*) shows z_{avs}/L_j and figure 3(*c*) shows z_{avs}/L_a.

For highly forced plumes ($\Gamma_0 \ll 1$, figure 3*b*) our solution (2.27) for the $\alpha = \gamma_1 + \gamma_2 Ri$ formulation clearly shows $z_{avs} \sim O(L_j)$, thereby confirming that the adjustment length does scale on the jet length. The distance between actual and virtual origins is less than that predicted by the Hunt & Kaye (2001) constant-α model. Note that (2.27) gives

$$\frac{z_{avs}}{L_j} = \frac{4}{3\kappa Ri_p^{1/2}} \cdot {}_2F_1\left(\frac{1}{2}; \frac{3}{8\gamma_2/\kappa - 10}; 1 + \frac{3}{8\gamma_2/\kappa - 10}; 1\right) \approx 0.58 \quad \text{for } \Gamma_0 \ll 1. \tag{4.1}$$

For highly lazy plumes ($\Gamma_0 \gg 1$, figure 3*c*), our solution (2.27) for the $\alpha = \gamma_1 + \gamma_2 Ri$ formulation shows that the adjustment length does not scale on the acceleration length scale (note the scale on the vertical axis). Instead, it follows from (2.27) that the virtual origin, and by extension also the adjustment length, scales on the plume radius at source

$$\frac{z_{avs}}{L_q} = \frac{4}{3\kappa Ri_p^{1/2}} \approx 3.34 \quad \text{for } \Gamma_0 \gg 1 \tag{4.2}$$

(see figure 3*a*). By contrast, the solution for the constant-α formulation, wherein $\zeta_{avs} \sim \Gamma_0^{-1/5}$, appears to scale well on the acceleration length. This apparent change in adjustment length (from L_a to L_q) has been observed in experimental measurements of highly lazy plumes (Kaye & Hunt 2009), where the transition to a volume flux that varies as a 5/3rds power law occurs downstream of the neck of the plume and is independent of Γ_0. The solution (2.27) and ζ_{avs} from Hunt & Kaye (2001) diverge as the acceleration length L_a decreases with increasing Γ_0.

5. Conclusions

Our focus has been on developing analytical solutions that are applicable to turbulent plumes from area sources for which entrainment, varying locally in response to the fluxes of momentum, volume and buoyancy, is characterised by an entrainment function α that is linearly dependent on the local Richardson number. This form for the entrainment underpins our developments as it has been shown, both experimentally and numerically, to universally capture the behaviour of forced, pure and lazy plumes. We derive analytical solutions for the virtual origin, the fluxes of momentum and volume and the local Richardson number without placing restrictions on the source conditions. Our solutions thereby encompass the entire spectrum of forced, pure and lazy plume releases.

For forced and lazy releases, we show how the dynamical conditions in the plume approach the far-field equilibrium state of a pure plume and that this approach is less rapid than predicted under the assumption of invariant entrainment, i.e. for the widely adopted simplification $\alpha = \text{constant}$. Our solutions indicate that forced plumes adjust to become pure plume-like within a streamwise distance comparable to 60 % of a source jet length, while lazy plumes adjust within a distance comparable to three source radii. Finally, our analytical solution for the virtual origin agrees closely with data that span five orders of magnitude of source Richardson number, thereby giving us confidence in the application of this solution to general plumes from area sources.

Acknowledgements

G.R.H. gratefully acknowledges the EPSRC through grant no. EP/N010221/1, entitled Managing Air for Green Inner Cities (MAGIC).

Declaration of interests

The authors report no conflict of interest.

Appendix A. The entrainment function of Carazzo *et al.* (2006)

Carazzo *et al.* (2006) propose an entrainment function in the form

$$\alpha = \gamma_1 + \gamma_2 Ri + \frac{\mathrm{d}\gamma_3}{\mathrm{d}\zeta}, \tag{A 1}$$

where γ_3 is a higher-order integral property that depends on the velocity, buoyancy and turbulent stress profiles. As noted by van Reeuwijk *et al.* (2016), the third term, $\mathrm{d}\gamma_3/\mathrm{d}\zeta$, compensates for the adjustment in velocity and buoyancy profiles and can, as a result, be neglected in a time-averaged analysis. Our solutions are consistent with the model (A 1) in that we specify that the profiles are assumed to be either top-hat or Gaussian.

Appendix B. Two-dimensional plumes

Defining a pure-plume Richardson number as $Ri_{0L} = B_{0L}Q_{0L}^3/M_{0L}^3$ and scaled source Richardson number as $\Gamma_{0L} = Ri_{0L}/2\alpha_p\kappa$, the conservation equations for a two-dimensional plume of dimensionless volume and momentum fluxes per unit length of the source, q_L and m_L, can be deduced to give

$$\frac{\mathrm{d}q_L}{\mathrm{d}\zeta_L} = \gamma_{1L}\frac{m_L}{q_L} + \gamma_{2L}Ri_{pL}\frac{q_L^2}{m_L^2} \quad \text{and} \quad \frac{\mathrm{d}m_L}{\mathrm{d}\zeta_L} = \kappa Ri_{pL}\Gamma_{0L}\frac{q_L}{m_L}, \tag{B 1a,b}$$

where $\zeta_L = zM_{0L}/Q_{0L}^2$. Combining (B 1*a*,*b*) one may obtain the solutions

$$q_L^3 = \frac{m_L^3}{\Gamma_{0L}} + \frac{\Gamma_{0L}-1}{\Gamma_{0L}}m_L^{6\gamma_{2L}/\kappa} \quad \text{and} \quad \Gamma_L = 1 + (\Gamma_{0L}-1)m_L^{6\gamma_{2L}/\kappa-3}. \tag{B 2a,b}$$

A virtual origin correction for a two-dimensional plume with a linear Ri entrainment function is reported in van den Bremer & Hunt (2014), their appendix A. Following the approach developed herein (§ 2), the correction can be expressed in terms of hypergeometric functions as

$$\zeta_{avs,L} = \frac{\mathscr{F}_{\delta,L}}{\kappa Ri_{pL}\Gamma_{0L}^{2/3}}, \tag{B 3}$$

where

$$\mathscr{F}_{\delta,L} = {}_2F_1\left(\frac{1}{3}; \frac{1}{6\gamma_{2L}/\kappa - 3}; 1 + \frac{1}{6\gamma_{2L}/\kappa - 3}; 1 - \Gamma_{0L}\right). \tag{B 4}$$

It should be noted that there is, as yet, no experimental evidence that supports the notion of a linear entrainment function for two-dimensional lazy plumes.

REFERENCES

ABRAMOWITZ, M. & STEGUN, I. 1964 *Handbook of Mathematical Functions*. US Government Printing Office.

BAINES, W. D. 1983 A technique for the direct measurement of volume flux of a plume. *J. Fluid Mech.* **132**, 247–256.

VAN DEN BREMER, T. S. & HUNT, G. R. 2014 Two-dimensional planar plumes and fountains. *J. Fluid Mech.* **750**, 210–244.

CARAZZO, G., KAMINSKI, E. & TAIT, S. 2006 The route to self-similarity in turbulent jets and plumes. *J. Fluid Mech.* **547**, 137–148.

EZZAMEL, A. 2011 Free and confined buoyant flows. PhD thesis, Imperial College London.

EZZAMEL, A., SALIZZONI, P. & HUNT, G. R. 2015 Dynamical variability of axisymmetric buoyant plumes. *J. Fluid Mech.* **765**, 576–611.

FISCHER, H. B., LIST, J. E., KOH, R. C. Y., IMBERGER, J. & BROOKS, N. H. 1979 *Mixing in Inland and Coastal Waters*. Academic Press.

HUNT, G. R. & VAN DEN BREMER, T. S. 2011 Classical plume theory: 1937–2010 and beyond. *IMA J. Appl. Maths* **76** (3), 424–448.

HUNT, G. R. & KAYE, N. G. 2001 Virtual origin correction for lazy turbulent plumes. *J. Fluid Mech.* **435**, 377–396.

HUNT, G. R. & KAYE, N. B. 2005 Lazy plumes. *J. Fluid Mech.* **533**, 329–338.

INCE, E. L. 1956 *Ordinary Differential Equations*. Dover.

KAMINSKI, E., TAIT, S. & CARAZZO, G. 2005 Turbulent entrainment in jets with arbitrary buoyancy. *J. Fluid Mech.* **526**, 361–376.

KAYE, N. B. 2008 Turbulent plumes in stratified environments: a review of recent work. *Atmos.-Ocean* **46** (4), 433–441.

KAYE, N. B. & HUNT, G. R. 2007 Overturning in a filling box. *J. Fluid Mech.* **576**, 297–323.

KAYE, N. B. & HUNT, G. R. 2009 An experimental study of large area source turbulent plumes. *Intl J. Heat Fluid Flow* **30** (6), 1099–1105.

MARJANOVIC, G., TAUB, G. N. & BALACHANDAR, S. 2017 On the evolution of the plume function and entrainment in the near-source region of lazy plumes. *J. Fluid Mech.* **830**, 736–759.

MORTON, B. R. 1959 Forced plumes. *J. Fluid Mech.* **5** (1), 151–163.

MORTON, B. R. & MIDDLETON, J. H. 1973 Scale diagrams for forced plumes. *J. Fluid Mech.* **58** (01), 165–176.

MORTON, B. R., TAYLOR, G. & TURNER, J. S. 1956 Turbulent gravitational convection from maintained and instantaneous sources. *Proc. R. Soc. Lond.* A **234** (1196), 1–23.

PAPANICOLAOU, P. N. & LIST, E. J. 1988 Investigations of round vertical turbulent buoyant jets. *J. Fluid Mech.* **195**, 341–391.

PRIESTLEY, C. H. B. & BALL, F. K. 1955 Continuous convection from an isolated source of heat. *Q. J. R. Meteorol. Soc.* **81**, 144–157.

VAN REEUWIJK, M. & CRASKE, J. 2015 Energy-consistent entrainment relations for jets and plumes. *J. Fluid Mech.* **782**, 333–355.

VAN REEUWIJK, M., SALIZZONI, P., HUNT, G. R. & CRASKE, J. 2016 Turbulent transport and entrainment in jets and plumes: a DNS study. *Phys. Rev.* F **1**, 1–25.

ROUSE, H., YIH, C. S. & HUMPHREYS, H. W. 1952 Gravitational convection from a boundary source. *Tellus B* **4** (3), 201–210.

THIELICKE, W. & STAMHUIS, E. J. 2014 PIVlab towards user-friendly, affordable and accurate digital particle image velocimetry in MATLAB. *J. Open Res. Softw.* **2**, 1–10.

TURNER, J. S. 1973 *Buoyancy Effects in Fluids*. Cambridge University Press.

TURNER, J. S. 1986 Turbulent entrainment: the development of the entrainment assumption, and its application to geophysical flows. *J. Fluid Mech.* **173**, 431–471.

WANG, H. & LAW, A. W. 2002 Second-order integral model for a round turbulent buoyant jet. *J. Fluid Mech.* **459**, 397–428.

WOODS, A. W. 2010 Turbulent plumes in nature. *Annu. Rev. Fluid Mech.* **42** (1), 391–412.